REMARKS

This Amendment is filed in response to the Office Action dated March 15, 2006. For the following reasons this application should be allowed and the case passed to issue. No new matter is introduced by this Amendment. The amendment to claim 7 is supported by the specification at page 9, lines 11-16 and Fig. 3.

Claims 1-20 are pending in this application. Claims 1-6 have been withdrawn pursuant to a restriction requirement. Claims 7-10 and 13-20 have been rejected. Claims 11 and 12 have been objected to. Claim 7 has been amended in this response.

Claim Rejections Under 35 U.S.C. §§ 102 and 103

Claims 7-9 and 13-16 were rejected under 35 U.S.C. § 102(e) as being anticipated by Nakamura et al. (U.S. Pat. No. 6,933,234).

Claims 9, 10, and 17-20 were rejected under 35 U.S.C. § 103(a) as being unpatentable over Nakamura et al.[1]

These rejections are traversed, and reconsideration and withdrawal thereof respectfully requested. The following is a comparison between the invention as claimed and the cited prior art.

An aspect of the invention, per claim 7, is a method of chamfering a nitride semiconductor wafer comprising the steps of preparing a soft whetting apparatus having a long continually-fed elastic matrix and whetting granules implanted on the matrix and bringing the elastic matrix into angular inscribing contact with an edge of the circular nitride wafer with an angular contact angle of 40 degreees to 90 degrees at a pressure. The matrix is supplied with a whetting liquid which is powderless water, powderless oil, powder including water, or powder

[1] In the Office Action claims 9, 10, and 17, and 18-20 were rejected in two separate rejections as obvious in view of Nakamura et al.

BEST AVAILABLE COPY

including oil. The nitride wafer is rotated in the inscribing contact with the elastic matrix. The elastic matrix is fed at a constant speed or varying speeds in the angular direction around the wafer edge. The edge of the wafer is abraded by the granules implanted on the soft matrix into edge roughness of Ra5μm to Ra10nm.

The purpose of the present invention is to smooth an edge of as-grown nitride round wafer. As-grown wafer is produced by growing nitride semiconductor crystal on a foreign undersubstrate, slicing the grown crystal and eliminating the foreign material undersubstrate. An as-grown wafer is polished into a "mirror wafer" and a variety of films are grown epitaxially on the mirror wafer to form an "epitaxial wafer". Electrodes are subsequently formed on the "epitaxial wafer" to form a "processed wafer." Thus, the wafers are changed from an as-cut wafer, via a mirror wafer and an epitaxial wafer to a processed wafer. An edge of the as-grown nitride semiconductor wafer (a beginning wafer) is polished by a tangentially-fed elastic material implanted with whetting granules in an inscribing contact with the edge of the object nitride wafer.

Nitride semiconductor wafers are harder and more fragile than silicon wafers. The edges of nitride wafers are more likely to break. Chamfering or beveling of edges is indispensable for ordinary semiconductor wafers. Chamfering is common to silicon wafers and GaAs wafers, but there is no known method for polishing edges of nitride wafers. It is not possible to directly transfer techniques of chamfering silicon wafers to nitride wafer is no use. Mechanical and chemical sturdiness of nitride semiconductors causes serious difficulties in chamfering. The edges of nitride wafers should be chamfered, since a sharp rough edge would break and invite fractures in wafer process. The method of the present invention includes a tangential contact and tangential feeding of an elastic matrix (whettape). Inscribing contact is a synonym of tangential

contact. The friction force between the elastic matrix and the edge is tangential. Tangential friction force does not break the edge of a fragile nitride wafer. The feeding of the elastic matrix invites an extra friction force. The feeding direction is tangential in the present invention. The additional, extra friction force does not break a fragile nitride wafer. The inner contact angle is wide for dispersing the friction force. The inner contact angle, according to the present invention, is 40 degrees to 90 degrees (page 19, line 16 of the written description). The wide contact alleviates the danger of cracking, breaking, or splitting. The tangential inscribing contact and the tangential feeding characterize the present invention.

Nakamura et al. goals are not to polish nitride wafers, not to polish as-grown wafers, and not to polish edges. Nakamura et al.'s objective is to eliminate acicular projections born at edges of processed silicon wafers. Nakamura et al. is directed towards processed wafers, not as-grown wafers. The wafers of Nakamura et al. have many memory units which have been made by a series of epitaxial growth, impurity doping, diffusion, capacitor production, electrode production, and wirings by a sequence of wafer processes. The processing produces acicular projections 94 on edges of silicon processed wafers. Nakamura et al. aim to eliminate acicular projections via polishing. Nakamura et al. disclose that the edge B on the wafer has been rounded by chamfering which is a step of making a mirror wafer, as shown in Fig. 17. Nakamura et al. further disclose (column 1, lines 35-44):

"In the present specification, for example, as shown in FIG. 17, a portion at the end of a principal surface of a wafer 90 where the edge line of the section of the wafer 90 cut along the center thereof is curved will be referred to as a bevel B. A substantially flat portion formed between the bevel B and the principal surface of the wafer 90 will be referred to as an edge E.

The width of the edge E is several mm. A portion including these bevel B and edge E will be referred to as a periphery in the present specification."

The smooth edge E has been already chamfered in the mirror-wafer making process. The step of chamfering has already been done in Nakamura et al. and the edge has been slantingly smoothed, as shown in FIG. 17. Since the Nakamura et al. process produces memory devices, Nakamura et al. try to make trench capacitors on the silicon wafer on which epitaxial films already have been piled and impurity has been doped by implantation or thermal diffusion. FIG. 17 shows a processed silicon wafer 90, SiN film 91, and SiO_2 film 92 coating the wafer 90. Hard mask (HM) (SiO_2/SiN) in is shown in Figs. 17-19. Six holes are formed on the HM mask for making trenches for memory capacitors. RIE (reactive ion etching) forms deep trenches 93 via the holes on the silicon wafer. The RIE, however, causes a side effect of shooting an object with halogen ions. Halogen ions bombard the holed mask 91/92 for boring deep trenches 93 in the silicon. The halogen ions attack the masked silicon wafer to make dust or reactants. The synthesized dust or reactants fall on the naked peripheries B and E and pile on the naked peripheries in of the wafers. The E/B becomes rough due to the deposition of the dust or reactants. The depositions make acicular projections 94 on the peripheries B/E. In other words, the acicular projections 94 are produced by the fall of reactants or dust produced by the halogen attack of the RIE on the masks 91 /92 as shown in FIG. 18. The depositions act as a mask for protecting Si peripheries, then acicular projections 94 are made.

As disclosed in column 1, lines 53-61, Nakamura et al. disclose:

"Subsequently, as shown in FIG. 18, the Si wafer 90 is etched using the hard mask HM serving as a mask by an RIE method, thus forming the deep trenches 93. At this time, generally, acicular projections 94 are generated in an area corresponding to the bevel B and the edge

portion E of the Si wafer 90. It is considered that a by-product generated in RIE is deposited on exposed surface of the bevel B and the edge E of the Si wafer 90, the by-product functions as a mask for etching, and the surface of the Si wafer 90 is etched."

One object of the Nakamura et al. process is to eliminate the acicular projections 94 which are a side-effect of RIE for forming capacitor trenches. Another purpose of Nakamura et al. is to eliminate Ru (ruthenium) depositions. Ru electrodes are new electrodes for capacitors. Some of the ruthenium atoms are deposited on the peripheries B/E contaminating the peripheries with Ru residue. Nakamura et al. aim to eliminate the residue of Ru which are deposited on the trenches for making electrodes of capacitors. Nakamura et al. teach (column 2, lines 44-51):

"In recent years, in the field of semiconductor devices, new materials such as Cu serving as a wiring material, Ru and Pt serving as capacitor electrode materials for a next-generation DRAM or FeRAM, and TaO and PZT serving as capacitor dielectric materials are introduced one after another. It is time to seriously consider about problems of contamination caused by these new materials in mass production."

Thus, Nakamura et al.'s polishing has two purposes. One is to eliminate acicular projections 94 produced by depositions of RIE on the edges of a processed silicon wafer. The other is to eliminate Ru residues produced by Ru (ruthenium) electrode production on trench capacitors. Trench capacitors are well-suited for high density memory device (DRAM). Capacitance of a capacitor C is in proportion to the area of a dielectric film. Therefore, horizontal capacitors occupy much area. However, DRAM technology of making large capacitance capacitors having deep vertical holes allows the coating holes with large area dielectric films. Therefore, the capacitance of the trench capacitors can be large.

The objects (aciculae and depositions), which have sizes of 1 nm to 10 nm, are far smaller than 1 μm order. The objects are laid on near horizontal peripheries, since the origins of the aciculae and dusts are depositions of halogen atoms and ruthenium atoms. Sizes of the depositions are on the order of 1 nm to 10 nm.

Nakamura et al. disclose (column 5, lines 27-38):

"According to the first embodiment, the thickness of the silicon nitride film 91 used to form the hard mask HM on the principal surface of the wafer 90 shown in FIG. 17, namely, the device surface is set to 200 nm. The thickness of the SiO_2 film 92 is set to 900 nm. In FIG. 18, the diameter of an aperture of each deep trench 93 formed using the hard mask HM is set to 0.25 μm and the depth thereof is set to 7 μm.

When the deep trenches 93 are formed using the hard mask HM shown in FIG. 17 by the RIE processing, the acicular projections 94 are formed on the periphery of the Si wafer 90 including the bevel B and the edge E on the principal surface side of the wafer 90."

Figs. 1A and 1B show the structure of a polishing machine of Nakamura et al. A silicon wafer 90 is sustained by four rollers la, lb, lc, and 1d, which rotate the wafer. Two equivalent abrasive tapes 2a and 2b are in contact with two spots on edges of the silicon wafer on a diameter. The abrasive tape 2a is pulled by a supply roller 2aRl and a take-up roller 2aR2 in FIG. 1. The tape moves from the supplying roller 2aRl downward round the edge to the take-up roller 2aR2. The tape rubs the edge vertically from top to bottom. The pulling force is given by the upper supplying-roller 2aRl and the take-up roller 2aR2. The contact between the tapes 2a, 2b and the edge of the wafer is not tangential but radial to the wafer. The contact is vertical, not horizontal but vertical. Radial/vertical contact characterizes Nakamura et al.. The object of whetting is not the sharp edge but the smoothly slanting periphery as shown in FIG. 1B.

To further distinguish the claimed invention from the prior art, FIG. A-H are attached in Appendix I. FIG. A and FIG. B show the Nakamura et al. process having a silicon wafer of a 300 mm diameter, a supply roller, and a radial-vertical contact whetting tape. The tape runs in a radial direction and passes the edge in a vertical direction. Nakamura et al.'s tape is in tight contact with an edge only at the middle of the tape. The silicon wafer rotates in an angular direction. Friction force acting upon the tape is vertical to the direction of feeding and supporting. If the sides of the tape were not supported, the tape would twist or whirl due to the angular friction force as shown in FIG. B. Thus Nakamura et al. push the tape by extra members 4a, 4b and 5a and 5b, as shown in Nakamura et al. FIG. 1B. The extra members prevent the tape from twisting and whirling. But if the silicon wafer rotation speed is increased, the tape twist/whirl would occur. The tape twist is a drawback of Nakamura et al. process.

FIG. C illustrates a partial section of the Nakamura et al. process. A supply roller dispenses the tape and a take-up roller pulls the tape and withdraws. The tape moves in the radial and vertical directions and the edge of the silicon wafer is pulled down by the feeding tape. The down-pulling force causes a downward shear stress on the wafer distorting the wafer. The wafer downward distortion is another drawback of the Nakamura et al. process.

FIG. D shows a plan view of the Nakamura et al. Si wafer and the whettape. O is a center of the silicon wafer. The silicon wafer has a diameter of 300 mm and a radius of 150 mm. OJ is a radius. EFG is a front side of the supply roller which is a starting position of the whettape. IJH is a tape-turnover line. K is the length of the whettape from the supply roller to the turn-over line IJH. W is the width of the tape. If the tape had no elasticity, only the middle point J would touch the wafer edge and sides I and H were untouched and separated from the edge. If the tape has sufficient elasticity, the sides I and H will be in weak contact. In FIG. D,

OV = OJ = OU = R, where R is a radius of the silicon wafer. IJH is vertical to OJ. $\angle VOU = \Theta$. $\angle VOJ = \Theta/2$. Gaps IV = UH = $R(1-\cos(\Theta/2))$. When Θ is large, the gaps IV and UH are large.

Nakamura et al. teach (column 12, line 57) that the width of the whetting tapes 2a and 2b is 3cm. The silicon wafer is a 300 mm diameter wafer (12 inch wafer).

"Each of the first and second abrasive films had a width of 3 cm. As shown in FIG. 3, around the wafer 90 of 300 m diameter, ..."

When the wafer radius is 15 cm and the tape width is 3 cm the contact angle of Nakamura et al. is $3/15 \times 180/\pi = 11.4°$. $\theta = 11.4°$, R = 150mm, Thus, Gaps IV = UH = 150 mm x (1-cos5.7d°) = 0.74 mm. There are 0.74 mm wide gaps IV and UH between the tape and the edge. Actual measurement teaches that K = 100 mm in FIG. 1A of Nakamura et al. and IV/K = 0.0074. Nakamura et al. disclose that the elasticity of the tape allows the sides of the tape to come into contact with the edge of the wafer.

For example, the Young modulus of polyethylene is 0.077×10^{11} dyn/cm^2 (770 MPa). The Young's modulus for high density polyethylene ranges from 621 MPa to 896 MPa. 770 MPa is selected as the middle of the handbook range of polyethylene. Nakamura et al. disclose the use of PET tape, but does not limit the tape to PET. Therefore, the tape of Nakamura et al. can be made of polyethylene, which is softer than PET. Therefore, the following calculations represent a best case for Nakamura et al. As PET is a harder material (its handbook value of Young's modulus ranges from 2760-4140 MPa). Therefore, there would be correspondingly less contact area than that which is calculated for polyethylene. Copies of the handbook values of Young's Modulus are attached in Appendix II.

Assuming that the tape of Nakamura may have Young's modulus 0.077×10^{11} dyn/cm^2. Forces should be applied to points I and H to cancel the gap IV and UH = 0.74 mm. Strain f,

Young's modulus E and the deformation ε (IV/K = 0.0074) satisfies f = Eε. The necessary strain f = 0.077 x 10^{11} dyn/cm^2 0.0074 = 5.7 x 10^7 dyn/cm^2 = 5.7 x 10^6 N/m^2 = 5.7 x 10^6 Pa = 56 atm = 58 kg/cm^2. The wafer thickness w and the tape thickness t is unknown in Nakamura. However 300 μm to 400 μm are general thickness of Si wafers. While recognizing that unless specifically stated, patent drawings can not be used for scaling dimensions, in view of Figs. 1B, 5, and 6c, and practical considerations it appears that the thickness of the whetting tape is 100 μm. Thus, it is reasonable to assume a ratio of thicknesses of the wafer to the tape (w/t) = 3.

If w/t = 3, the pressure which should be applied to the edge of the wafer by the tape tension is 58 kg/cm^2/3 = 19.3 kg/cm^2. This is a calculated pressure applied to the edge of the wafer for expanding the middle FJ to cancel gaps VI and UH in FIG. D. Nakamura et al., however, only apply a pressure of 1 kg/cm^2 to the edge/tape interface (see column 11, lines 25-26). Nakamura et al.'s pressure is about 1/20 of the necessary pressure for eliminating the gaps VI and UH in FIG. D. The pressure (1 kg/cm^2) is too weak to expand the tape to cancel the gaps IV and HU in FIG. D. Thus, the gaps IV and HU are maintained in Nakamura.

How much tape deformation at an application of a pressure of 1 kg/cm^2 is now calculated. The Young modulus of the tape is E = 0.077 x 10^{11} dyn/cm^2 (polyethylene) and f = Kε. If f = 1 kg/cm^2 = 980000 dyn/cm^2 = 9.8 x 10^5 dyn/cm^2, ε = 9.8 x 10^5 dyn/cm^2/0.077x10^{11} dyn/cm^2 = 1.27 x 10^{-4}. Since K = 100 mm, a deformation length is 100 mm x 1.27 x 10^{-4} = 1.27 x 10^{-2} mm. The pressure 1 kg/cm^2 expands the 100 mm long tape by only 1.27 x 10^{-2} mm. The small scope of expansion essentially means there is a point contact (J point) of Nakamura et al. The angle θ of the contact region satisfies an equation R(1-cos(θ/2)) = Δ. Δ is a reduction of 1.27 x 10^{-2} mm, R = 150 mm, and θ = 2cos^{-1}{1-(Δ/R)} = 2cos^{-1} {1-(0.0127/150)} = 1.5 degrees. Thus, the contact angle is only 1.5 degrees in Nakamura et al. The contact width is Rθ = 150

mm x 1.5π/180 = 4 mm. Although the Nakamura et al. tape has a 3 cm width, the actual contact region has a 4 mm width. An extra 26 mm width of the tape separates from the edge in Nakamura et al. The insufficient contact is a further drawback of the Nakamura et al. process. The drawbacks originate from Nakamura et al.'s vertical, radial contact of the tape.

In the Nakamura et al. process, only the middle point J is in a tight contact and the sides I and H separate. The pressure is non-uniform. If the calculated 19.3 kg/cm^2 is applied to the edge of the wafer, the pressure is non-uniform. The pressure is the highest at J falls to zero at the sides I and H. The right hand graph shows a pressure on the edge, when the applied pressure is 19.3 kg/cm^2. The non-uniform pressure is a further drawback of the Nakamura et al. process. Four drawbacks of Nakamura have been described: twist of tap, distortion of wafer, insufficient contact, and non-uniform pressure.

The present invention, on the other hand, features tangential/horizontal/angular contact of tape to the wafer. The contact angle is 40 degrees to 90 degrees of an angular width, while the Nakamura et al. contact angle is 11 degrees (an actual contact angle is 1.5°). Thus, the contact angle of the present invention is 4 times to 8 times as large as Nakamura et al.

The contact angle of Nakamura et al. is actually smaller than 11 degrees. Since the tape vertically passes wafer from top via the edge to bottom, the middle of the tape is in tight contact with the wafer, but the sides of the tape are separated from the edge. Very strong elastic deformation allows the sides of the tape to very weakly touch the wafer. The tape pressure acting on the edge by the tape is not uniform in the angular direction in Nakamura et al. The reasons of the insufficient contact and the non-uniform pressure of the tape derive from the vertical/radial contact of Nakamura et al. Nakamura et al. disclose only 1 kg/cm^2 pressure which causes a narrow 1.5° contact. The claimed contact angle (40 to 90 degrees) is 26 times to 60

times as large as the Nakamura et al. actual contact angle. This is a very large and unobvious difference.

Further, in the present invention the tangential contact allows the tape to contact in a constant pressure to the wafer edge. As shown in FIG. E, the tape is in horizontal/angular/ tangential contact with the edge. The force acting on the edge is a radial force. FIG. F illustrates that there is no occurrence of shear stress. The tangential contact realizes a uniform pressure acting on the edge from the tape. FIG. G shows the uniform-pressure with the arrows showing the strength of the pressure. The wide contact angle of 40 degrees to 90 degrees ensures smooth polishing of the edge of the wafer. The present invention employs a wide inner contact of 40 degrees to 90 degrees as shown in Fig. 3 and disclosed at page 10, lines 11-15:

"The whettape inscribes an edge of a wafer, which increases a contact length and reduces the force per unit area. Such features of the whettape reduce the probability of splitting, scratching or breaking in chamfering steps and enhance the final obtainable edge smoothness to Ra10nm to Ra 100nm."

The wide contact area of 40 degrees to 90 degrees reduces the pressure and reduces the probability of breaks of wafers.

In paragraph 3 of the Office Action the Examiner asserted:

"Nakamura et al. (USPN 6,933,234) ... bringing the tape 2a into inscribing contact with an edge of the circular wafer 90 at a pressure, ..."

However, Nakamura et al. do not bring the wafer edge into inscribing contact with the tape. Nakamura et al.'s contact is not inscribing, but rather vertical contact. The vertical feeding of Nakamura invites downward shear stress to the object wafer. The strong shear stress by the vertical feeding could break a GaN wafer, since a GaN wafer is far fragile than a silicon wafer.

The present invention employs an angular inscribing contact. As shown in FIG. E, the feeding according to the present invention does not cause shear stress in an object wafer. A fragile GaN wafer would not be broken by the feeding operation in the present invention. Thus Claim 7 is not suggested by Nakamura et al. Nakamura et al.'s contact angle is 11 degrees at most. In practice, the vertical contact reduces the contact angle to less than 11 degrees in Nakamura et al. The tape goes from the top via an edge to the bottom of an object wafer. The middle of the tape is pulled by a strong force, but the sides of the tape are relaxed and separated from the wafer.

As regards claims 9,10 and 17, the Examiner acknowledged that Nakamura et al. do not disclose the feed speed of the tape is 5 mm/min to 60 mm/min and the contact between the wafer edge and the tape has a wide angle area of 40 degrees to 90 degrees. It would have been obvious to one having ordinary skill in the art at the time the invention was made to select the feed speed of the tape is 5 mm/min to 60 mm/min, the contact between the wafer edge and the tape has a wide angle area of 40 degrees to 90 degrees, since it was held that where the general conditions of a claim are disclosed in the prior art, discovering the optimum or workable ranges involves only routine skill in the art.

Contrary to the Examiner's assertions, Nakamura et al. do not suggest the claimed feed speed and contact angle. FIG. H denotes a virtual tape polishing machine of Nakamura et al. having 90 degrees contact angle. EFG is a supply-roller and EFG-HJI is a tape. The tape turns downward on the reverse surface. $\angle VOU = 90$ degrees and the tape runs from EFG to IJH. J is in contact with the edge of a Si wafer of a 300 mm diameter and O is a center of the Si wafer. $OV = OJ = OU = 150$ mm, $\angle VOJ = \angle UOJ = 45°$, And $EG = VU = IH = 2R\sin 45° = 2 \times 150$ mm $\times \sin 45° = 212$ mm.

If Nakamura et al. would employ 90 degrees of angular inscribing contact, the tape would have a width of 150 mm x 2 x sin45° = 212 mm. FIG. H shows a virtual Nakamura et al. apparatus. Instead of a 3 cm wide tape, Nakamura would have to employ a 21.2 cm wide tape for obtaining a 90 degree inscribing contact angle. If Nakamura adopted a 212 mm wide tape which is in vertical contact with the wafer edge, almost all of the tape would separate from the edge of a wafer. Only a middle J point of the tape would maintain contact. If the pressure of the tape at the middle point J is 1 kg/cm^2, the contact length is only 4 mm near J. If the pressure of the tape at the middle point J is 19 kg/cm^2, the contact width is 30 mm as calculated before.

In FIG. H, the gaps IV = 150 mm x (1-cos45°) = 43.9 mm. If a large pressure is applied to the tape by the roller at EFG for canceling the gaps IV and HU, the deformation ratio ε would be ε = 43.9 mm/100 mm = 0.43. $E = 0.077 \times 10^{11}$ dyn/cm^2, $f = E\varepsilon$, $f = 0.077 \times 10^{11}$ $dyn/cm^2 \times 0.43 = 3.3 \times 10^9$ $dyn/cm^2 \times 3.3 \times 10^8 N/m^2 = 3.3 \times 10^8 Pa$ = 3300 atm = 3300 kg/cm^2. This value is 3300 times stronger than the 1 kg/cm^2 disclosed by Nakamura et al. Namely almost all of the sides 1J and HJ are separated from the edge. As illustrated by the virtual model having a 90 degree wide of a tape as shown in FIG. H it is clear that Nakamura et al. would not suggest the claimed method to one skilled in the art, since almost all of the tape are inactive and useless. Clearly the claimed method are not anticipated or obvious in view of Nakamura et al.

The dependent claims are allowable for at least the same reasons as claim 7, and further distinguish the claimed method.

Allowable Subject Matter

Claims 11 and 12 are objected to as being dependent upon a rejected base claim but would be allowable if rewritten in independent form.

Applicants gratefully acknowledge the indication of allowable subject matter. Because it is believed that claim 7 is allowable for the reasons explained above it is not believed that further amendment of the claims is necessary.

In view of the above amendments and remarks, Applicants submit that this application should be allowed and the case passed to issue. If there are any questions regarding this Amendment or the application in general, a telephone call to the undersigned would be appreciated to expedite the prosecution of the application.

To the extent necessary, a petition for an extension of time under 37 C.F.R. § 1.136 is hereby made. Please charge any shortage in fees due in connection with the filing of this paper, including extension of time fees, to Deposit Account 500417 and please credit any excess fees to such deposit account.

Respectfully submitted,

McDERMOTT WILL & EMERY LLP

Bernard P. Codd
Registration No. 46,429

600 13th Street, N.W.
Washington, DC 20005-3096
Phone: 202.756.8000 BPC:MWE
Facsimile: 202.756.8087
Date: July 17, 2006

Please recognize our Customer No. 20277 as our correspondence address.

APPENDIX I

FIG.A

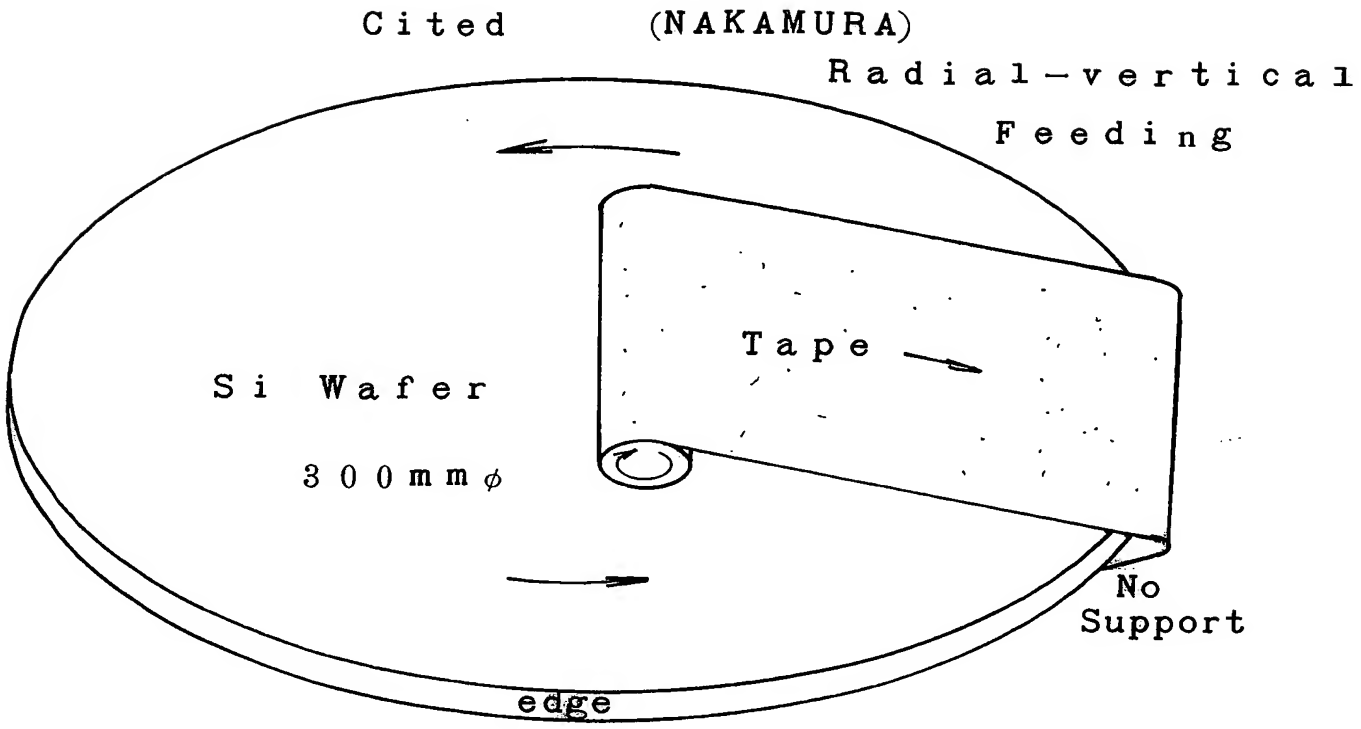

FIG.B

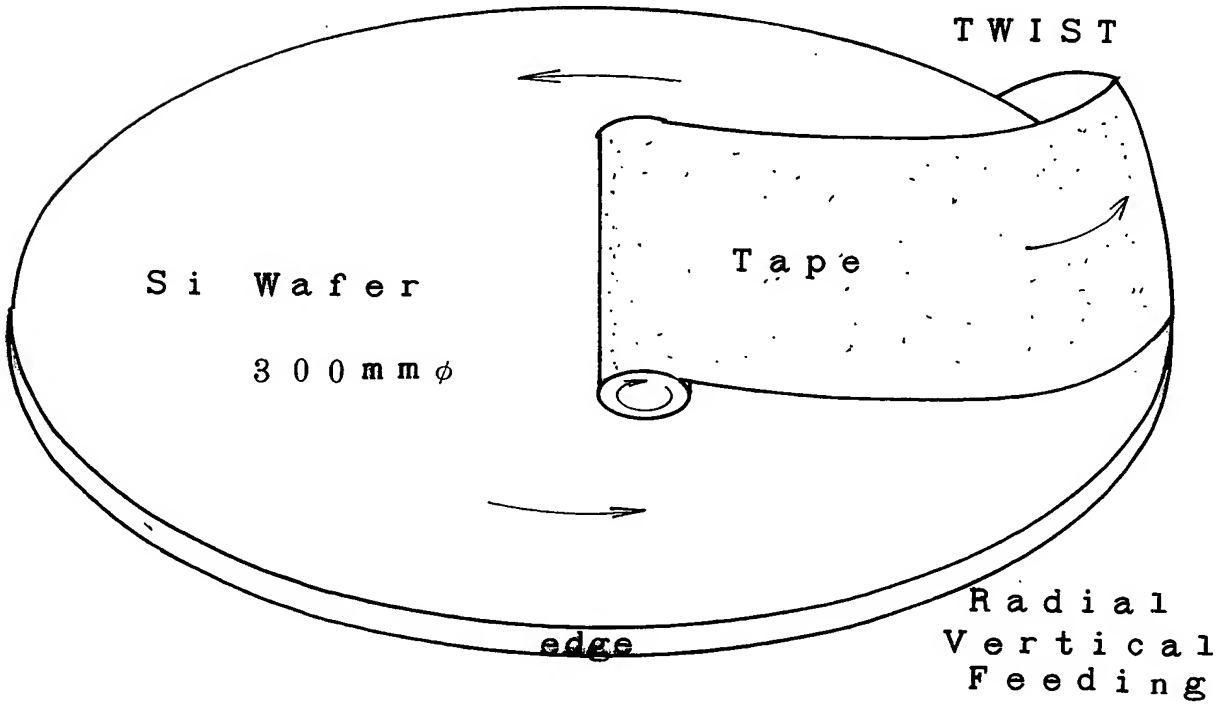

APPENDIX I

FIG. C

Cited NAKAMURA

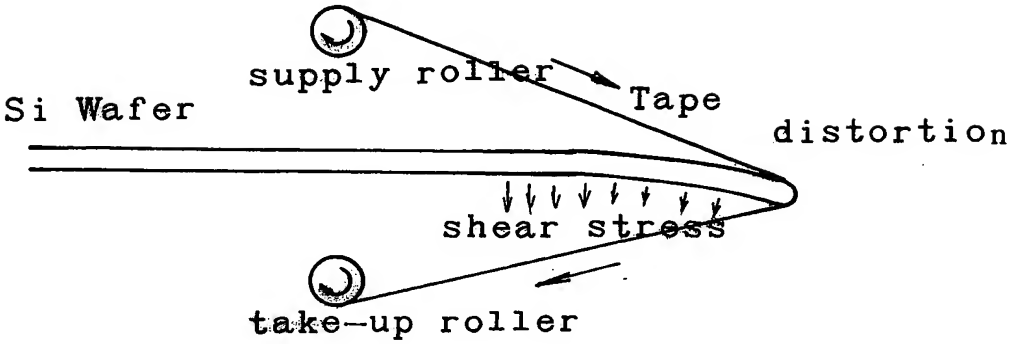

FIG. D

Cited NAKAMURA

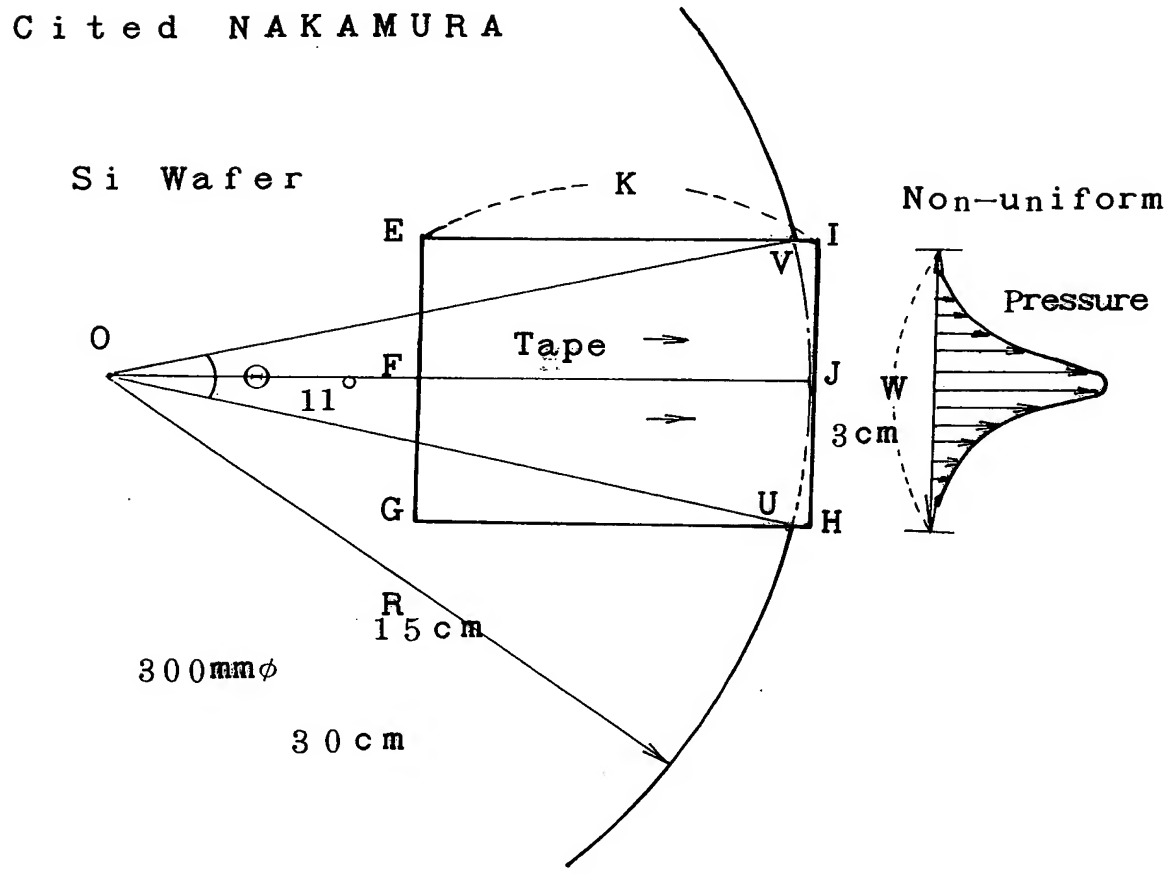

FIG. E

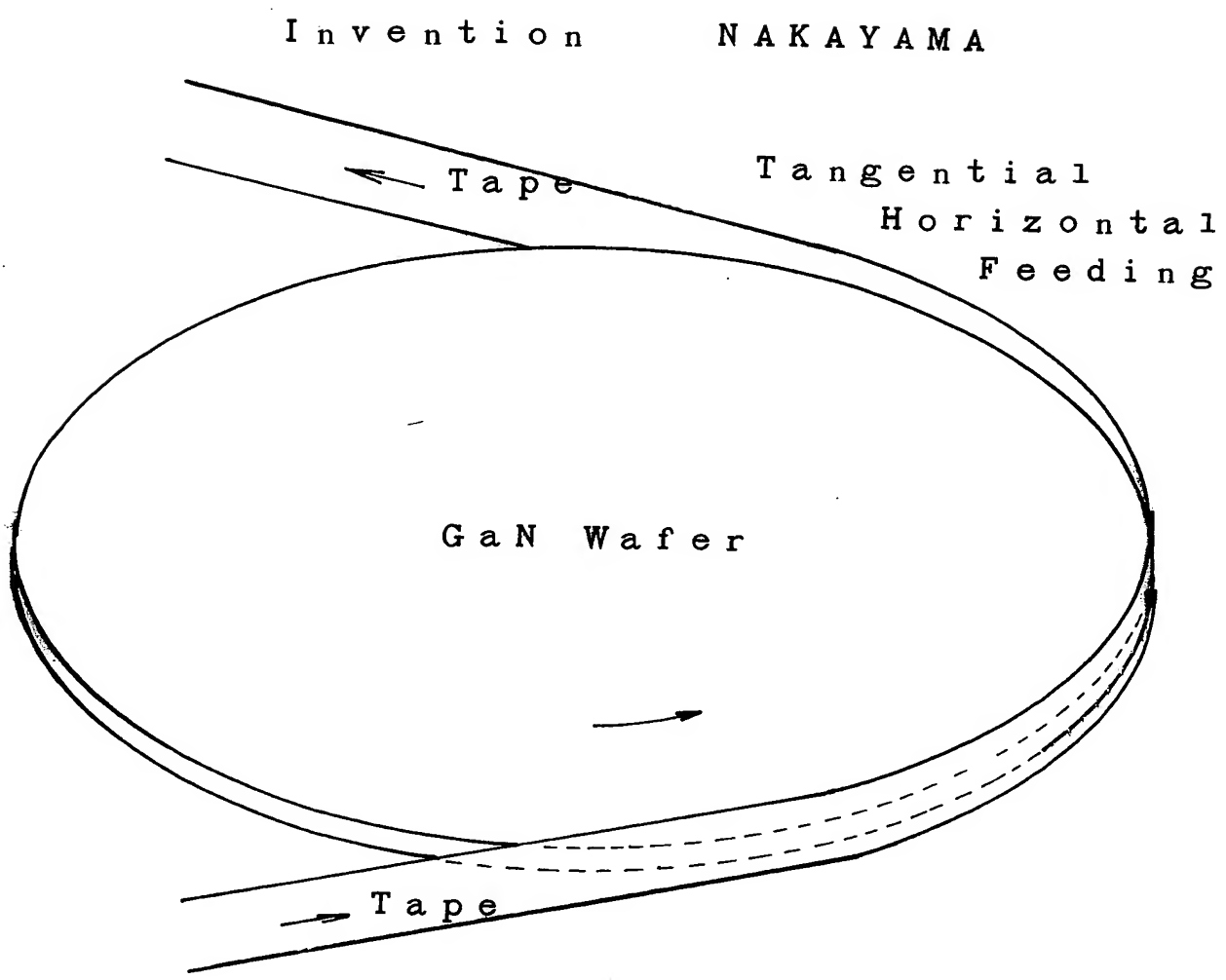
Invention
NAKAYAMA
Tape
Tangential
Horizontal
Feeding
GaN Wafer
Tape

FIG. F

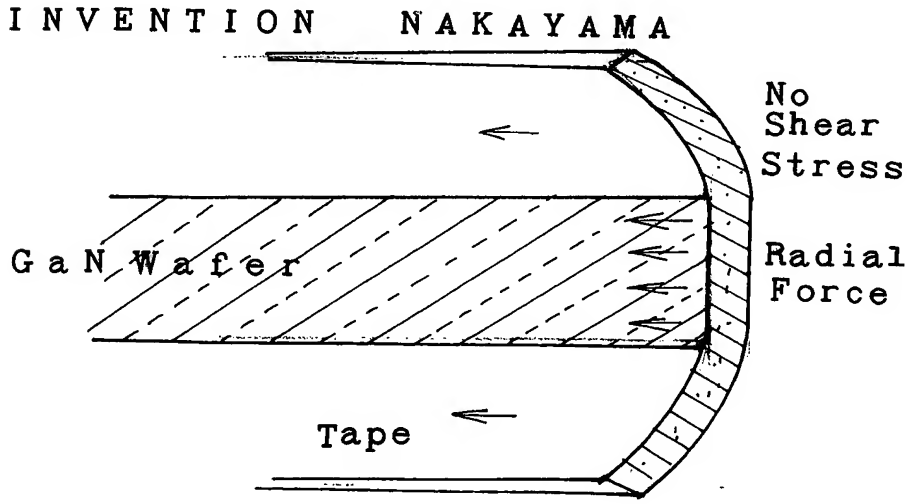
INVENTION
NAKAYAMA
No
Shear
Stress
GaN Wafer
Radial
Force
Tape

APPENDIX I

FIG. G

INVENTION

NAKAYAMA

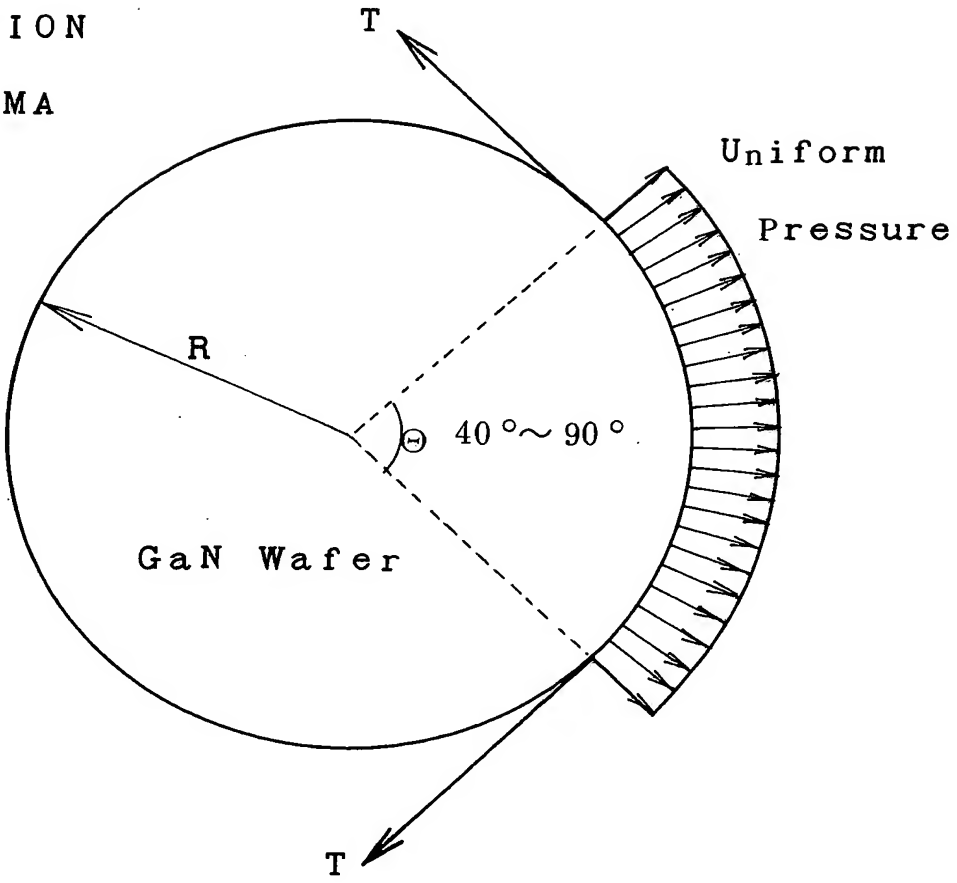

FIG. H

Cited NAKAMURA

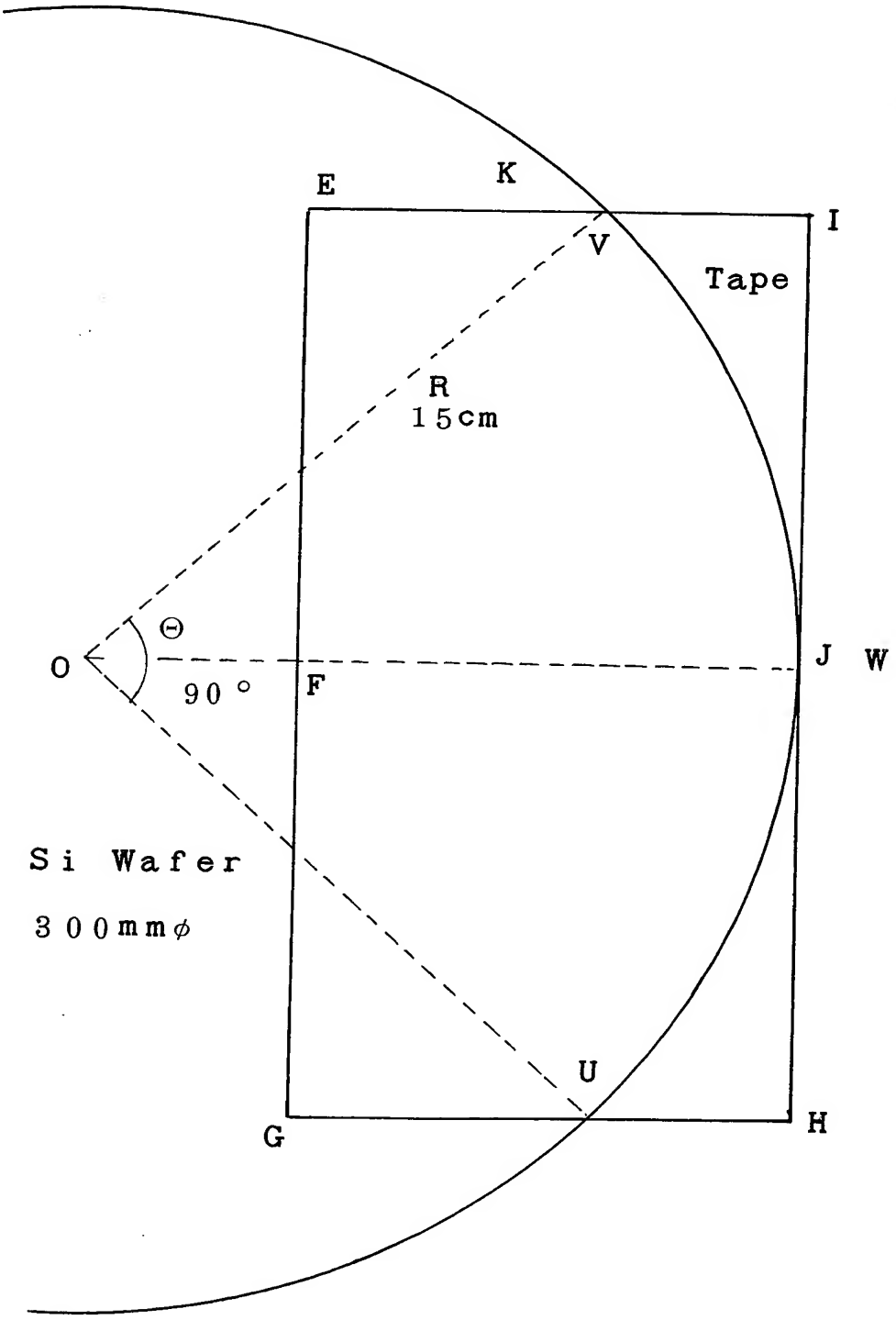

APPENDIX II

3.1.2.1 種々の結晶の弾性率 [10^{11}dyn/cm^2]

(1) 立方晶系結晶

固体	C_{11}	C_{44}	C_{12}	温度	固体	C_{11}	C_{44}	C_{12}	温度
Ag	12.40	4.61	9.34		CuZn	12.91	8.24	10.97	
Al	10.82	2.85	6.13		Fe_3O_4	27.3	9.7	10.6	
Au	18.6	4.20	15.7		FeS_2	36.2	10.4	−4.4	
C	110	44	33		GaAs	1.192	0.538	0.599	
Cu	16.84	7.54	12.14		GaSb	8.85	4.33	4.04	
Ge	12.89	6.71	4.83		InSb	6.72	3.02	3.67	
K	0.457	0.263	0.374	83 K	KBr	3.46	0.505	0.58	
Li	1.48	1.08	1.25	78 K	KCl	3.98	0.625	0.62	
Mo	46	11.0	17.6		KI	2.67	0.421	0.43	
Na	0.945	0.618	0.779	−183°C	LiF	11.77	6.28	4.33	
Ni	24.65	12.47	14.73		MgO	28.6	14.8	8.7	
Pb	4.66	1.44	3.92		NH_4Br	2.96	0.53	0.59	
Si	16.57	7.96	6.39		NH_4Cl	3.90	0.68	0.72	
Th	7.53	4.78	4.89		NaBr	3.87	0.97	0.97	
W	50.1	15.14	19.8		$NaBrO_3$	5.73	1.52	1.76	
AgBr	5.63	0.720	3.3		NaCl	4.87	1.26	1.24	
AgCl	6.01	0.625	3.62		$NaClO_3$	4.99	1.17	1.41	
$Ba(NO_3)_2$	5.93	1.21	1.89		PbS	12.7	2.48	2.98	
CaF_2	16.44	3.47	5.02		TlBr	3.78	0.756	1.48	
Cr_2FeO_4	32.3	11.4	14.4		TlCl	4.01	0.760	1.53	
Cu_3Au	19.07	6.63	13.83		ZnS	10.79	4.12	7.22	

(2) 六方晶系結晶

固体	C_{11}	C_{33}	C_{44}	C_{12}	C_{13}	温度
Be	28.1	30.2	15.5	−2.5		
Cd	12.1	5.13	1.85	4.81	4.42	
Co	30.7	35.81	7.53	16.5	10.3	
H_2O	1.384	1.499	0.319	0.707	0.581	−16°C
Mg	5.97	6.17	1.64	2.62	2.17	
SiO_2	11.66	11.04	3.606	1.67	3.28	600°C
Zn	16.1	6.10	3.83	3.42	5.01	

(3) 正方晶系結晶

固体	C_{11}	C_{33}	C_{44}	C_{66}	C_{12}	C_{13}	温度
In	4.45	4.44	0.655	1.22	3.95	4.05	
Sn	7.35	8.7	2.2	2.265	2.34	2.8	

(4) 三方晶系結晶

固体	C_{11}	C_{33}	C_{44}	C_{12}	C_{13}	C_{14}	温度
Al_2O_3	46.5	56.3	23.3	12.4	11.7	10.1	
Bi	6.28	4.40	1.08	3.50	2.11	−0.42	
$CaCO_3$	13.74	8.01	3.42	4.40	4.50	−2.03	
Fe_2O_3	24.2	22.8	8.5	5.5	1.6	−1.3	
Hg	3.60	5.05	1.29	2.89	3.03	0.5	−190°C
$NaNO_3$	8.67	3.74	2.13	1.63	1.60	0.82	
Sb	7.92	4.27	2.85	2.48	2.61	1.05	
SiO_2	8.76	10.68	5.72	0.607	1.33	1.73	35°C

APPENDIX II

3.1.2.2 種々の固体の等方弾性率

固　　体	ヤング率, E [10^{11}dyn/cm²]	剛性率, G [10^{11}dyn/cm²]	ポアソン比, σ
アルミニウム	6.8	2.4～2.5	0.355
ベリリウム	31	14.7	0.05
黄銅（Cu 70, Zn 30）	10.5	3.8	0.374
銅	12.6	4.6	0.37
ジュラルミン	7.14	2.67	0.335
金	8.1	2.85	0.42
電解鉄	21	8.2	0.29
鉛	1.5	0.54	0.43
マグネシウム	4.23	1.62	0.306
ニッケル	21.4	8.0	0.336
白　金	16.8	6.4	0.303
銀	7.5	2.7	0.38
ステンレススチール	19.7	7.57	0.30
す　ず	5.4	2.08	0.34
タングステン	36.2	13.4	0.35
亜　鉛	10.5	4.2	0.25
溶融石英	7.3	3.12	0.17
パイレックスガラス	6.2	2.5	0.24
重シリカフリントガラス	5.3	2.18	0.224
軽ボレートクラウンガラス	4.6	1.81	0.274
ルサイト	0.39	0.143	0.4
ナイロン	0.35	0.122	0.4
ポリエチレン	0.077	0.026	0.458
ポリスチレン	0.36	0.133	0.353

PE

3.1.2.3 合金の弾性率，降伏応力，かたさ

（1） アルミニウム合金 [dyn/cm²]

合金の組成 [%]	ヤング率, E	剛性率, G	降伏応力	ブリネルかたさ
Al 99.996	6.89×10^{11}	2.65×10^{11}	1.22×10^{8}	17
Al 99.0	6.89×10^{11}	2.65×10^{11}	3.45×10^{8}	23
Al, 1.2 Mn	6.89×10^{11}	2.65×10^{11}	4.14×10^{8}	28
Al, 5.5 Cu, 0.5 Pb, 0.5 Bi	7.10×10^{11}	2.65×10^{11}	32.4×10^{8}	95
Al, 4.4 Cu, 0.8 Si, 0.8 Mn, 0.4 Mg（アニール）	7.31×10^{11}	2.65×10^{11}	9.65×10^{8}	45
（時効）*	7.31×10^{11}	2.65×10^{11}	41.4×10^{8}	135
Al, 4 Cu, 0.5 Mg, 0.5 Mn（アニール）	7.17×10^{11}	2.65×10^{11}	6.89×10^{8}	45
（時効）*	7.17×10^{11}	2.65×10^{11}	27.6×10^{8}	105
Al, 4 Cu, 2 Ni, 0.5 Mg（時効）*	7.10×10^{11}	2.65×10^{11}	32.4×10^{8}	115
Al, 4.5 Cu, 1.5 Mg, 0.6 Mg（時効）*	7.31×10^{11}	2.65×10^{11}	31.7×10^{8}	120
Al, 4.5 Cu, 0.8 Mn, 0.8 Si（時効）*	7.17×10^{11}	2.65×10^{11}	24.1×10^{8}	110
Al, 12.5 Si, 1.0 Mg, 0.9 Cu, 0.9 Ni（時効）*	7.10×10^{11}	2.65×10^{11}	31.7×10^{8}	125
Al, 1.0 Si, 0.6 Mg, 0.25 Cr（時効）*	7.03×10^{11}	2.65×10^{11}	27.6×10^{8}	100
Al, 1.3 Mg, 0.7 Si, 0.25 Cr（時効）*	6.89×10^{11}	2.65×10^{11}	13.8×10^{8}	65
Al, 1.0 Mg, 0.6 Si, 0.25 Cu, 0.25 Cr（時効）*	6.89×10^{11}	2.65×10^{11}	14.5×10^{8}	65
Al, 5.5 Zn, 2.5 Mg, 1.5 Cu, 0.3 Cr, 0.2 Mn（時効）*	7.17×10^{11}	2.65×10^{11}	49.6×10^{8}	150

*印は時効硬化状態．

APPENDIX II

表 23　各種ラミネート紙の主な特性例一覧表（厚さ150μm 担当）[39]

	項目	SIOLAP	PPLP	PML	FEP/C	クラフト紙
プラスチック特性	CH結合による分類	ポリオレフィン			非ポリオレフィン	—
	プラスチック材料と分子構造	グラフト架橋ポリエチレン（架橋 PE）	ポリプロピレン（PP）	ポリメチルペンテン（TPX）	ふっ化エチレンプロピレン共重合体(FEP)	天然繊維
		$-(CH_2-CH_2)_n-$	$-(CH_2-CH(CH_3))_n-$	$-(CH_2-CH(CH_2-CH(CH_3)_2))_n-$	$-(CF_2-CF_2)_x-(CF_3-CF(CF_3))_y-_n$	
	密度 (g/cm³)	0.94～0.965	0.90～0.92	0.83～0.84	2.12～2.17	
	気中融点 (℃)	128～130	165～176	236	275	
	DDB中融点 (℃) (N_2ガス雰囲気DSCによる)	124～125	135	161	—	
	誘電率(商用周波)	2.25～2.35	2.2～2.3	2.12	2.1	
	誘電正接(商用周波) (%)	<0.05	<0.05	<0.09	<0.03	
	引張強さ (kg/cm²)	200～400	250～350	245～280	200～250	
	伸び (%)	200～1,000	200～700	10～50	250～350	
	熱伝導率 (cal/cm·s·℃)	8×10^{-4}	3×10^{-4}	4×10^{-4}	6×10^{-4}	5×10^{-4}
絶縁体	構造	クラフト紙／架橋PE／クラフト紙	クラフト紙／PP／クラフト紙	クラフト紙／TPX／クラフト紙	クラフト紙／FEP／クラフト紙	クラフ
	製法	押出ラミネート	押出ラミネート	押出ラミネート	熱カレンダ	—
	$\varepsilon\times\tan\delta$ (%) (80℃)	2.8×0.08	2.8×0.08	2.7×0.072	2.5×0.05	3.2×0.17
	AC（シート） (kV/mm)	118	135	118	104	80
	インパルス(シート) (kV/mm)	260	250	214	229	150
	密度 (g/cm³)	0.93	0.88	0.79	1.65	0.6
	気密度 (G·s)	∞	∞	∞	∞	1,400
	引張強さ (kg/mm²)	6.7	5.9	6.3	5.6	5～6
	伸び (%)	3.5	2.5	4.3	2.7	3.2
	膨潤(絶乾ベース100℃) (%)	3.6	4	3.9	≒0	—
	85～100℃aging 後はく離強度 (g/15mm 幅)	はく離不可	80	80	はく離不可	—

(ハ)　ラミネート紙　セルロース紙とプラスチックフィルムを積層して一体化した複合絶縁紙である。プラスチックの高い絶縁破壊の強さと，小さい誘電特性を利用したもので，油の含浸性をセルロース紙で補った電力ケーブル用絶縁紙である。

その多くは，1枚のプラスチックフィルムを2枚のクラフト紙で両側からはさんだ構造であり，プラスチック層としてはポリプロピレン，架橋ポリエチレン，ふっ化エチレンプロピレン共重合体，ポリ4-メチルペンテン-1などが用いられる。これらのラミネート紙のプラスチック層の化学構造と特性およびラミネート紙になったときの構造と特性を表23[39]に示す。

この結果，従来のクラフト紙に比べて，これらのラミネート紙の絶縁破壊の強さは大きく，誘電率，誘電正接は小さい。例えばポリプロピレンとクラフト紙の複合であるポリプロピレンラミネート紙の雷インパルス，商用周波における絶縁破壊の強さは，いずれも従来のクラフト紙より60%大きい。また，ポリプロピレンラミネート紙の誘電損失は，従来のクラフト紙の約40%となり，誘電体による損失電力を大幅に低減することができる[40]。

これらのラミネート紙は，国内・国外において275～500 kV級のOFケーブルに実用化されはじめ，現在のところ，ポリプロピレンラミネート紙がほぼ主流を占めている[41][42]。

（2）　繊　　維[43]　天然繊維と化学繊維に大別される。天然繊維は自然界で繊維の形をしているものをそのまま糸にしたもので，綿，絹，麻などがある。化学繊維には合成繊維，再生繊維，半合成繊維がある。合成高分子を繊維にしたのが合成繊維である。天然繊維を一度化学薬品（水酸化ナトリウム，二硫化炭素）に溶解したのち，化学構造を変化させることなく糸にした繊維がコースレーヨンなどの再生繊維である。天然繊維の骨格の一部化学処理により異なった構造にした繊維がアセテートなどの成繊維である。

これらの繊維は，ワニスと組み合わせたワニスクロス，エポシ樹脂，フェノール樹脂と組み合わせた積層板，ゴムと組みせた絶縁テープおよび半導電性テープなどに用いられる。このかにも介在物，集合材料など，電気電子機器の補助材料として用されている。

合成繊維には，ポリアミド(ナイロン)，ポリエステル，ニルアルコール，ポリアクリロニトリル，ポリオレフィンウレタン，ポリフルオロエチレン，ポリ塩化ビニル，ポリ塩化ニリデンなどがあり，工業用材料として広く用いられている。

このほか，最近，機械的特性に優れ高い弾性率をもつや超延伸により分子鎖を一方向に配向させた超高力ポリエなどがある。

（b）　熱可塑性樹脂材料[44]～[47]　分子鎖や線状の高分子逆的に，温度が高くなると融解して流動しやすくなり(塑性冷却すると硬くなる。この性質を熱可塑性という。熱硬化

APPENDIX II

表 24

熱可塑性樹脂の性質[44]（I）

	試験法 (ASTM)	ポリエチレン						ポリプロピレン		塩化ビニル樹脂	
		LDPE (MDPE)	L-LDPE	HDPE (ホモ)	HDPE (共重合)	EVA	EEA	PP (ホモ)	PP (共重合)	PVC (硬質)	PVC (軟質)
融点(ガラス転移点) (℃)	——	106～115	122～124	130～137	125～132	103～108		168	160～168	(75～105)	(75～105)
引張破壊強さ (MPa)	D638	8～31	13～28	22～31	21～45	15～28	11～14	31～41	28～38	41～52	10～24
引張破壊伸び (%)	D638	100～650	100～950	10～1,200	10～1,300	300～750	700～750	100～600	200～700	40～80	200～450
引張降伏強さ (MPa)	D638	9～14	10～19	26～33	18～29	8～41		31～37	24～30		
圧縮破壊(降伏)強さ (MPa)	D695			19～25	19～25		21～25	38～55	26～55	55～90	6～12
破壊(降伏)時曲げ応力 (MPa)	D790							41～55	34～48	69～110	
引張弾性率 (MPa)	D638	172～283	262～517	1,070～1,090	621～896	48～200	28～52	1,140～1,550	689～1,170	2,410～4,140	
圧縮弾性率 (MPa)	D695							1,030～2,070			
曲げ弾性率(MPa) 23℃	D790	241～331	276～517	1,000～1,550	827～1,240	53		1,170～1,720	896～1,380	2,070～3,450	
93℃								345	276		
121℃								241	207		
149℃											
アイゾット衝撃値 (ft·lb/in)	D256A	破壊せず	1.0～9.0	0.4～4.0	0.35～6.0	破壊せず	破壊せず	0.4～1.0	1.0～20.0	0.4～20	材料により広範囲に変化
ロックウェル硬さ	D785							R80～102	R50～96		
ショア硬さ	D2240	D44～50		D66～73	D58～70	D17～45	D27～28			D65～85	A50～100
線膨張係数 (10^{-6}/K)	D696	100～220		59～110	70～110	160～200	160～250	81～100	68～95	50～100	70～250
熱変形温度(℃) 1.8MPa	D648							49～60	46～60	60～77	
0.5MPa		40～44		79～91	65～80			107～121	85～104	57～82	
熱伝導率 (W/(m·K))	C177	0.33		0.46～0.50	0.42			0.12	0.15～0.17	0.15～0.21	0.13～0.17
比重	D792	0.917～0.932	0.918～0.935	0.952～0.962	0.939～0.960	0.922～0.943	0.93	0.900～0.910	0.890～0.905	1.30～1.58	1.16～1.35
吸水率(%) 3.2mm厚さ24時間	D570	<0.01		<0.01	<0.01	0.05～0.13	0.04	0.01～0.03	0.03	0.04～0.4	0.15～0.75
3.2mm厚飽和											
絶縁破壊強さ(MV/m) 3.2mm厚 短時間法	D149	18～39		18～20	18～20	24～30	18～22	24	24	14～20	12～16

	ポリスチレン		ポリカーボネート	ポリアミド樹脂				ポリエステル樹脂		ふっ素樹脂	
	PS (一般用)	PS (耐衝撃用)	PC	6-ナイロン	66-ナイロン	11-ナイロン	12-ナイロン	PET	PBT	PTFE	PFA
融点(ガラス転移点) (℃)	(100～105)		(150)	210～220	265	191～194	176～179	254～259(73)	232～267	327	310
引張破壊強さ (MPa)	36～52	19～43	66		83(76)	55	55～62(55)	59～72	57	14～34	28～30
引張破壊伸び (%)	1.2～2.5	20～60	110	30～100(300)	60(300)	300	300	50～300	50～300	200～400	300
引張降伏強さ (MPa)		19～41	62	81(51)	55(45)						
圧縮破壊(降伏)強さ (MPa)	83～90		86	90～110	103(降伏)			76～103	59～100	12	
破壊(降伏)時曲げ応力 (MPa)	69～101	31～57	93	108(40)	117(42)			97～124	83～115		
引張弾性率 (MPa)	2,280～3,280	1,650～2,550	2,380	2,620(689)		1,280	1,240	2,760～4,140	1,930	400～552	
圧縮弾性率 (MPa)	3,310～3,380		2,410	(1,720)		1,240				414	
曲げ弾性率(MPa) 23℃	2,620～3,380	1,790～2,480	2,340	2,690(965)	2,900(1,280)	1,030	1,030～1,140	2,410～3,100	2,280～2,760	552	827
93℃			1,900								
121℃			1,690								
149℃											
アイゾット衝撃値 (ft·lb/in)	0.35～0.45	0.95～3.5	16(3.2mm)	0.6～1.0 (3.0)	0.8～1.0 (2.1)	1.8	2.0～2.5	0.25～0.65	0.8～1.0	3	破壊せず
ロックウェル硬さ	M60～75	L50～82	M70	R119	R120 M83	R108	R106～109 (R105)	M94～101	M68～78		
ショア硬さ										D50～55	D64
線膨張係数 (10^{-6}/K)	50～83		68	80～83	80	100	100	65	60～95		
熱変形温度(℃) 1.8MPa	77～94	77～96	132	68～85	75	54	52～54	38～41	50～85		
0.5MPa	68～96	74～93	138	185～191	246	149	145		116～191	121	74
熱伝導率 (W/(m·K))	0.13		0.20	0.24	0.24	0.33	0.22～0.31	0.15	0.18～0.29	0.25	0.25
比重	1.04～1.05	1.03～1.06	1.2	1.12～1.14	1.13～1.15	1.03～1.05	1.01～1.02	1.34～1.39	1.31～1.38	2.14～2.20	2.12～2.17
吸水率(%) 3.2mm厚24時間	0.01～0.03	0.05～0.07	0.15	1.3～1.9	1.0～1.3	0.3	0.25～0.30	0.1～0.2	0.08～0.09	<0.01	0.03
3.2mm厚飽和	0.01～0.03			8.5～10.0	8.5		0.9				
絶縁破壊強さ(MV/m) 3.2mm厚 短時間法	20～23		15	16	24	17	18		17～22	19	20

(注) ( ) 内は相対湿度50%の吸湿時の特性。

This Page is Inserted by IFW Indexing and Scanning Operations and is not part of the Official Record.

BEST AVAILABLE IMAGES

Defective images within this document are accurate representations of the original documents submitted by the applicant.

Defects in the images include but are not limited to the items checked:

- ☑ BLACK BORDERS
- ☐ IMAGE CUT OFF AT TOP, BOTTOM OR SIDES
- ☐ FADED TEXT OR DRAWING
- ☐ BLURRED OR ILLEGIBLE TEXT OR DRAWING
- ☐ SKEWED/SLANTED IMAGES
- ☐ COLOR OR BLACK AND WHITE PHOTOGRAPHS
- ☐ GRAY SCALE DOCUMENTS
- ☐ LINES OR MARKS ON ORIGINAL DOCUMENT
- ☐ REFERENCE(S) OR EXHIBIT(S) SUBMITTED ARE POOR QUALITY
- ☐ OTHER: _____

IMAGES ARE BEST AVAILABLE COPY.
As rescanning these documents will not correct the image problems checked, please do not report these problems to the IFW Image Problem Mailbox.